Author Manuscript

# A statistical study of poleward traveling ionospheric disturbances over the African and American sectors during geomagnetic storms

**John Bosco Habarulema[1,2], Golekamang P. Thaganyana[1,2], Zama T Katamzi-Joseph[1,2], Endawoke Yizengaw[3], Mark B. Moldwin[4], and Chigomezyo M. Ngwira[5]**

[1]South African National Space Agency (SANSA), Hospital Road, Hermanus 7200, South Africa.

[2]Department of Physics and Electronics, Rhodes University, 6140 Grahamstown, South Africa.

[3]Space Science Application Laboratory, The Aerospace Corporation, El Segundo, CA, USA.

[4]Department of Climate and Space Sciences and Engineering, University of Michigan, Ann Arbor, Michigan, USA.

[5]Atmospheric and Space Technology Research Associates, Louisville, CO, USA.

**Key Points:**

- Storm-time related poleward TIDs originating from the geomagnetic equatorial region occur mainly during local daytime.
- Large scale poleward TIDs are observed during the main phase while medium scale TIDs dominate the recovery phase, at least over the African sector.
- Increased vertical $\mathbf{E} \times \mathbf{B}$ drift plays a crucial role in launching poleward TIDs.

Corresponding author: John Bosco Habarulema, jhabarulema@sansa.org.za



This is the author manuscript accepted for publication and has undergone full peer review but has not been through the copyediting, typesetting, pagination and proofreading process, which may lead to differences between this version and the Version of Record. Please cite this article as doi: 10.1029/2021JA030162.

This article is protected by copyright. All rights reserved.

Author Manuscript

**Abstract**

We present statistical results of traveling ionospheric disturbances (TIDs) with origin near the geomagnetic equator during geomagnetic storms that occured within the period of 2010-2018. Based on storm criteria of Kp>4 and Dst$\leq -50$ nT, we have analyzed total electron content (TEC) perturbations derived from Global Navigational Satellite Systems (GNSS) observations within latitude range of 40°S-60°N and longitude ranges of $20°-40°$E; and $50°-70°$W representing the African and American sectors. Although the northern hemispheric part of the African sector has limited data coverage, results show that the launched TIDs do not exceed latitudinal distance of $20-25°$ from their origin during the analyzed period. A statistically similar result is observed over the American sector with launched poleward TIDs constrained largely within $\pm 20-30°$ around the geomagnetic equator. Where data are available, majority of these cases are linked to changes in ionospheric electrodynamics especially the enhancement of equatorial electrojet (EEJ), although there are other observations which are not explained by EEJ variability. This indicates that there may be other physical mechanisms that play a role in launching TIDs at the geomagnetic equator during disturbed conditions. An important result is that large scale and medium scale TIDs have been found to occur predominantly during the main and recovery phases of geomagnetic storms, respectively, at least over the African sector.

## 1 Introduction

Traveling ionospheric disturbances (TIDs) during geomagnetic storms are usually associated with solar wind - magnetosphere -ionosphere coupling that leads to the surge in the generation of atmospheric gravity waves (AGWs) as a result of enhanced Lorentz coupling, Joule heating and particle precipitation in auroral/high latitude regions [e.g., *Hunsucker*, 1982; *Hajkowicz and Hunsucker*, 1987; *Hocke and Schlegel*, 1996; *Balthazor and Moffett*, 1997; *Bruinsma and Forbes*, 2009]. Large scale TIDs (LS TIDs) show a dominant equatorward direction from both northern and southern hemispheres and have been extensively reported from ground-based instrumentation such as ionosondes and other radar systems [e.g., *Hocke and Schlegel*, 1996; *Nicolls et al.*, 2004; *Shiokawa et al.*, 2002], optical instruments such as airglow imagers [e.g., *Shiokawa et al.*, 2002] and satellite observations from different missions such as CHAMP, SWARM and general GNSS networks [*Bruinsma and Forbes*, 2009; *Tsugawa et al.*, 2004, 2003; *Nicolls et al.*, 2004; *Borries et al.*,



This article is protected by copyright. All rights reserved.

Author Manuscript

2009; *Katamzi and Habarulema*, 2014; *Habarulema et al.*, 2018]. Equatorward TIDs have been reported to cross either the geomagnetic or geographic equator to either hemisphere [e.g. , *Balthazor and Moffett*, 1997; *Bruinsma and Forbes*, 2009] in which case they could become poleward meaning that they are traveling in the poleward direction. Medium scale TIDs (MS TIDs) occur more frequently and are associated with many sources such as tropospheric and mountaneous turbulent processes [e.g., *Valladares and Hei*, 2012], and can propagate in any direction. MS TIDs have periods and velocities in the ranges of about 15-60 minutes and 100-250 m/s, respectively [e.g., *Kersley and Hughes*, 1989; *Hunsucker*, 1982]. Most LS TIDs have periods larger than 1 hour and velocities of 300-1000 m/s, although some studies have indicated the period range as 30 minutes to 3 hours [e.g., *Hocke and Schlegel*, 1996; *Hunsucker*, 1982]. Thus, there is sometimes "overlap" in either period or velocity values in classfying MS TIDs and LS TIDs. However, these types of TIDs originating from high/auroral regions as well as medium scale TIDs that do not have a preferred direction are not the focus of this paper.

Instead, we focus on TIDs which have been observed to have their origin from around the geomagnetic equator and propagate poleward during geomagnetic storms. Despite their possible existence having been suggested and numerically shown about 50 years ago [*Chimonas*, 1969; *Knudsen*, 1969], literature about their observations is nearly non-existent. This is because AGWs generated through equatorial electrojet (EEJ) dynamics and electrodynamics are difficult to observe and track due to their small amplitudes compared to the ones that originate from auroral regions [*Knudsen*, 1969]. It is only recently that these TIDs have started receiving attention with their existence having been reported in *Habarulema et al.* [2015] during the geomagnetic storm of 9 March 2012. Prior to this, *Ding et al.* [2013] showed poleward LS TIDs over China during the recovery phase of the 27 May - 01 June 2011 geomagnetic storm and attributed these observations to medium scale TIDs dissipating energy resulting into excitation of LS TIDs. Following *Habarulema et al.* [2015], it was further shown that poleward TIDs could be a result of enhanced EEJ during local daytime over the African and American sectors [*Habarulema et al.*, 2016]. Since then, a few studies have reported some aspects related to poleward TIDs possibly originating from the geomagnetic equator [e.g., *Habarulema et al.*, 2018; *Ngwira et al.*, 2019] and deep convection within the troposphere [e.g., *Jonah et al.*, 2018]. Recently, *Ngwira et al.* [2019] showed that while the TIE-GCM model clearly captured equatorward LS TIDs, it was unable to reveal the existence of MS TIDs of equatorial origin over Brazil-



This article is protected by copyright. All rights reserved.

Author Manuscript

ian longitudes during the storm of 22-23 June 2015. This leads to a number of scenarios including the possibility of the observed poleward TIDs being interhemispheric TIDs which may be amplified as they cross the geomagnetic equator, similar to results reported in *Pradipta et al.* [2016].

It is in this context that we perform a statistical study to determine the frequency of occurrence of poleward TIDs with specific emphasis on the ones originating from the geomagnetic equator during geomagnetic storms by analysing TEC within 2010-2018. Using the storm criteria of Kp>4 and Dst$\leq -50$ nT, we have analyzed 2-dimensional (2-D) maps of diurnal variability of TEC perturbations during geomagnetic storms occurring from 2010-2018. For this analysis, we have considered GNSS receiver locations within latitude range of 40°S-60°N and longitude ranges of 20°$-$40°E and 50°$-$70°W over the African and American sectors, respectively.

## 2 Data sources and method

In this study, observations of poleward TIDs are solely based on TEC derived from GNSS data within latitude and longitude ranges of 40°S-60°N and 20°$-$40°E; and 40°S-60°N and 50°$-$70°W over the African and American sectors, respectively. Over the GNSS receiver locations within the specified latitude and longitude ranges, TEC data were derived using the Boston College algorithm which has been utilized extensively in different TEC investigations [e.g., *Valladares et al.*, 2009; *Habarulema et al.*, 2016; *Pradipta et al.*, 2016, and some references therein].

Figure 1(a) shows the location of GNSS receivers (blue dots) used in this study, which reflects lack of sensors on the western part of the African continent that informed the choice of the 20°$-$40°E longitude sector represented within the vertical red lines. In an effort to minimize errors related to multipaths, we use TEC values with an elevation angle cutoff of 20° [e.g., *Habarulema et al.*, 2016]. To detect poleward TIDs, we apply a fourth-order polynomial fit to TEC for all satellites visible over all GNSS locations within the selected latitude and longitude ranges. The fitting procedure removes diurnal variability from the TEC segment time series data [e.g., *Valladares et al.*, 2009] and the difference between TEC and corresponding fits yields TEC perturbations (hereafter referred to as $\Delta$TEC). Figures 1(b)-(d) shows examples of $\Delta$TEC as a function of latitude and time for 16 July 2012, 14 April 2014 and 16 November 2014, respectively within



This article is protected by copyright. All rights reserved.

Author Manuscript

latitude and longitude ranges of 40°S-60°N and 20°−40°E. In Figures 1(b)-(d), the horizontal line depicts the geomagnetic equator at approximately 10° geographic latitude. For demonstration purposes, Figure 1(b)-(d) shows linear fits (represented by red lines) on traces of enhanced ΔTEC starting at approximately 0700 UT, 0530 UT and 1530 UT, respectively; which in this case act as estimated launching times of the associated poleward TIDs. With reference to the geomagnetic equator (horizontal red dashed line at 10°N, geographic), the fits in both southern and northern hemispheres appear nearly symmetric especially for Figures 1(b)-(c) signifying that the source mechanism for these TIDs may be around the equatorial region. Based on the linear fits, the velocity of the TIDs in Figures 1(b)-(d) have been determined using the gradient method [*Liu et al.*, 2019; *Thaganyana et al.*, 2021] as 380±33 m/s, 222±18 m/s and 348±5 m/s, respectively.

Figure 2 is similar to Figure 1, but for the American sector. The red vertical lines in Figure 2(a) show the latitude and longitude ranges used in the analysis. The horizontal red dashed line in Figures 2(b)-(d) depict the approximate location of the geomagnetic equator at 3°S geographic latitude. In Figures 2(b)-(d), ΔTEC (TECU) as a function of latitude and time within the 20 degrees longitude range covering 50°−70°W are shown for 02 October 2013, 15 July 2013 and 02 March 2017, respectively, from where poleward TIDs can be observed to be emerging at around 2100 UT, 1800 UT and 1700 UT. The determined velocity values for the fitted TID traces in Figures 2(b)-(d) are 240± 55 m/s, 330 ± 20 m/s and 282 ± 16 m/s, respectively.

## 3 Results and Discussion

Figure 3 shows statistical results of poleward TIDs launched from the geomagnetic equator over the African sector during the main and recovery phases of geomagnetic storms occuring from 2010-2018. Figure 3(a), shows the approximate time in different years at which poleward TIDs emerge as a function of the computed velocity. Results are presented for main (blue dots) and recovery (black crosses) phases. The main result or finding from Figure 3(a) is that these poleward TIDs were mainly observed in 2012 and 2015. Figures 3(b)-(c) show aggregated diurnal results of poleward TIDs' velocity (m/s) and period (hours) for main and recovery phases respectively. In Figures 3(b)-(c), velocities and periods of the TIDs are plotted as blue dots and open black circles, respectively, while the dashed vertical black lines represent the local sunrise (0700 LT) and sunset (1800 LT) times. In both phases, poleward TIDs are observed within time periods of 0400-1530



This article is protected by copyright. All rights reserved.

Author Manuscript

UT (about 0600-1730 LT) especially during local daytime. Following the period range categorization of 30 minutes to 3 hours for LS TIDs [e.g., *Hunsucker*, 1982; *Kersley and Hughes*, 1989], we found that almost all poleward TIDs (with exception of one case) during the main phase of geomagnetic storms were large scale with velocities ranging from $\simeq 300 - 550$ m/s. Apart from two cases, Figure 3(b) shows that period values range from 0.5-2 hours. During the recovery phase (Figure 3(c)), 63% and 37% of the observed poleward TIDs accounted for medium and large scale TIDs with period (velocity) ranges of 23-50 minutes (190-290 m/s) and 30 minutes -1.5 hours (300-410 m/s) respectively.

Figure 4 is similar to Figure 3 but for the American sector. The dashed vertical black lines in Figures 4(b)-(c) also represent the approximate local sunrise (0700 LT) and sunset (1800 LT) times. We observe fewer poleward TIDs over the American sector than in the African sector. Overall, there were about 12 and 40 identified cases of poleward TIDs over the American and African sector, respectively. A common finding is that poleward TIDs are to a large extent, a daytime phenomenon, an indication that their launching source mechanisms may be related or even similar. Results during the main phase (Figure 4(b)) show that the TIDs were mainly large scale with periods and velocity ranges of 45 minutes - 1.5 hours and 300-350 m/s (except one case), respectively. Out of the five cases observed during the recovery phase (Figure 4(c)), three fell within the MS TIDs category. Excluding the case which is very close to the 0700 LT line in Figure 4(b), there were three cases of poleward TIDs observed over the American sector during nighttime.

It has been suggested and numerically shown that changes in EEJ can have an influence in contributing to AGWs during disturbed conditions [e.g., *Knudsen*, 1969; *Chimonas*, 1969]. The possibility of these AGWs leading to poleward TIDs as a result of Lorentz coupling of ions to neutrals through collisions has been reported using TEC observations for two geomagnetic storms of 09 March 2012 and 17 March 2015 [*Habarulema et al.*, 2015, 2016, 2018]. To investigate the role played by changes in electrodynamics in contributing to these poleward TIDs, we statistically analyse the variability of EEJ during geomagnetic storms with reference to monthly median EEJ values for the month during which the storm occurred. The EEJ is computed from horizontal component (H) of Earth's magnetic field using a pair of magnetometer locations at the geomagnetic equator and another one displaced from the equator by 6-9 degrees following the well established differential magnetometer approach [*Rastogi and Klobuchar*, 1990; *Anderson et al.*, 2002, 2004; *Yizengaw et al.*, 2012]. Within our 20−40°E longitude sector over the African



This article is protected by copyright. All rights reserved.

Author Manuscript

region, the two magnetometer locations satisfying the need to apply differential magnetometer approach are Addis Ababa, AAE (9.0°N, 38.8°E; 0.2°N geomagnetic) and Adigrat, ETHI (14.3°N, 39.5°E; 6°N geomagnetic). The differential magnetometer approach first needs the correction of individual magnetometer observations for different offsets, which was done by subtracting daily average H values during 2300-0300 LT [e.g., *Yizengaw et al.*, 2011]. Once the offset correction on each magnetometer observation has been done, direct subtraction of the resulting H values gives $\Delta$H which is well known as the proxy of EEJ and is directly proportional to vertical $\mathbf{E} \times \mathbf{B}$ drift [*Anderson et al.*, 2004; *Yizengaw et al.*, 2012]. Additional details about the differential magnetometer approach can be found in several sources [e.g., *Rastogi and Klobuchar*, 1990; *Anderson et al.*, 2004; *Yizengaw et al.*, 2012, and references therein].

To determine the correlation between changes in EEJ and occurrence of poleward TIDs, we identify times of maximum $\Delta$H (EEJ) during the time range when poleward TIDs were observed. The database of $\Delta$H (EEJ) depends on availability of magnetometer data over two locations. Unfortunately, data over ETHI are only available from 2008-2013, limiting our ability to compute $\Delta H$ (EEJ) during the periods when we observed poleward TIDs especially in 2015. Thus, out of 14 and 26 cases where traces of poleward TIDs were identified during main and recovery phases, respectively it was only possible to determine $\Delta$EEJ for 11 comprising 5 and 6 cases during main and recovery phases, respectively.

Figure 5 shows an example of the method followed to identify maximum $\Delta$H during the time period when poleward TIDs existed for 11 March 2012 over the African sector. A similar approach was applied for all time periods and events when poleward TIDs were observed over both the African and American sectors. As a first step to suggest that the EEJ variability may have an impact on the origin of poleward TIDs, the $\Delta$H during the time duration of poleward TIDs existence should be above quiet time variability. During geomagnetic storms, this situation can be caused by additional contribution of electric field of magnetospheric origin [e.g., *Fejer and Scherliess*, 1995; *Huang et al.*, 2005] to the existing eastward electric field during local daytime in the equatorial regions. The enhanced eastward electric field then leads to increased Lorentz force that later makes coupling of the neutrals to ionized components effective for conditions responsible for launching poleward TIDs [*Chimonas*, 1969; *Habarulema et al.*, 2016]. In this study, we have determined the quiet time reference based on monthly median $\Delta$H. Figure 5(a) shows



This article is protected by copyright. All rights reserved.

Author Manuscript

the 2-D ΔTEC as a function of latitude and time for 11 March 2012. Traces of poleward TIDs are observed during 1000 - 1100 UT. Figure 5(b) shows changes in ΔH (EEJ, plotted in blue) for 11 March 2012 with monthly median ΔH (red curve) for March 2012. As represented between two vertical black lines, we observe a clear increase of ΔH over the corresponding monthly median values during 1000-1100 UT. The inset of Figure 5(b) shows the zoomed in variability of ΔH during this time interval. For the determination of correlation between the EEJ variability and occurrence of poleward TIDs, we select the time corresponding to maximum ΔH (during the time period when poleward TIDs are observable), which is 1033 UT as shown by the black dot in the inset of Figure 5(b). Figure 5(c) shows the correlation between the time corresponding to maximum ΔH (EEJ) and approximated start time of TIDs' observation during the time range when poleward TIDs were observed to be originating from the geomagnetic equator for all the 11 cases when data were available over the African sector. With this limited dataset, there is a clear one-to-one correlation between the launching of poleward TIDs from the geomagnetic equator and enhancement of EEJ as quantified by ΔH above the quiet time background monthly median ΔH.

Over the African sector, we have observed a single case where poleward TIDs existed during the time when ΔH (where available) showed a counter electrojet (CEJ) on 16 July 2012. Figure 6(a) shows the latitude-time plot of ΔTEC where traces of poleward TIDs are clearly visible starting at around 0700 UT (0900 LT). The red fitted lines show the orientation of the poleward TIDs in both southern and northern hemispheres. This particular TID occured during the recovery phase of the 15-16 July 2012 storm and fell within medium scale category based on its velocity and period values of 380 m/s and 32 minutes respectively. Figure 6(b) shows changes in ΔH (blue curve) on 16 July 2012 with monthly median ΔH (red curve). Despite some missing data, where available, ΔH is largely negative during 0700-0800 UT. At this point, we are unable to conclude whether there was increased EEJ responsible for this TID due to the existing data gap. Nevertheless, we see other traces of poleward TIDs between 0800-1000 UT coinciding with increased ΔH on 16 July 2012 over the respective monthly median ΔH values as shown by the inset figure in Figure 6(b).

Finally, Figure 7 is similar to Figure 5, but over the American sector. The ΔTEC - latitude plot as a function of time is shown for 02 March 2017 in Figure 7(a) from where poleward TIDs are visible starting at around 1700 UT (1300 LT). ΔH (blue curve) and



This article is protected by copyright. All rights reserved.

Author Manuscript

monthly median (red curve) for 02 March 2017 and March 2017, respectively are plotted in Figure 7(b). Increased ΔH (EEJ) is observed during the 1700-1800 UT period of poleward TID observation. ΔH reached a value of 37.89 nT at 1706 UT as shown by the black dot in the inset of Figure 7(b). Figure 7(c) shows the scatter plot of approximate occurrence times of poleward TIDs and the time corresponding to maximum ΔH (when EEJ on a geomagnetic storm day was above the respective monthly median) within the time range when the TIDs were present over the American sector. The pair of magnetometer locations within 50−70°W are Alta Floresta, ALTA (9.9°S, 56.1°W, 0.8°N geomagnetic) and Cuiaba, CUIB (15.6°S, 56.1°W, 5.9°S geomagnetic). However, ALTA-CUIB had significant missing EEJ data including for 2017, and therefore, the EEJ (ΔH) information shown in Figure 7(b) is for locations over Belem station, BELM (1.45°S, 48.5°W, 1.05°S geomagnetic) and Petrolina station, PETR (9.5°S, 40.5°W, 6.95°S geomagnetic). For cases in 2017 where EEJ data for ALTA-CUIB were not available, we have used EEJ data for BELM-PETR. The ALTA-CUIB and BELM-PETR pairs belong to LISN [*Valladares and Chau*, 2012] and AMBER [*Yizengaw and Moldwin*, 2009] networks respectively.

Returning to the scatter plot in Figure 7(c), the black dots are for ΔH data over ALTA-CUIB (and BELM-PETR for 2017 cases). For the three cases when EEJ data were available, ΔH was elevated above quiet time variability showing a correlation close to one. Due to the limited data set over ALTA-CUIB, we repeated a similar analysis using data for Jicamarca, JICA (11.8°S, 77.2°W; 0.8°N geomagnetic) and Piura, PIUR (5.2°S, 80.6°W; 6.8°N geomagnetic) and results are plotted in red crosses in Figure 7(c). As observed, both JICA-PIUR and ALTA-CUIB results are in agreement in showing that the occurrence of poleward TIDs has a high correlation with increased EEJ (ΔH) over the expected quiet time variability.

Our statistical results show that the storm induced poleward TIDs emerging from the equatorial regions are largely constrained within ±10−30° around the geomagnetic equator over both African and American sectors. In their analysis of properties of traveling atmospheric disturbances (TADs) during storms of 2001-2007, *Bruinsma and Forbes* [2009] stated that few cases of poleward TADs were observed, but did not propagate far from their source and were difficult to be tracked. With respect to TIDs of geomagnetic equator origin, the difficulty in tracking AGWs which give rise to poleward TIDs was earlier pointed out due to their lower amplitudes compared to those from auroral regions



This article is protected by copyright. All rights reserved.

Author Manuscript

[*Knudsen*, 1969] and thus require a relatively dense network of sensors such as GNSS receivers. This raises a question about the extent of spatial propagation of the launched AGWs and their associated physical mechanisms. If Lorentz coupling is the source mechanism of these AGWs in equatorial regions, why are the resulting TIDs not detectable away from low latitudes such as in mid latitudes as is the case with their auroral region related counterparts? The answer to this question lies partly in the orientation of the Lorentz force driving the ion-neutral collisions at equatorial and auroral regions. Due to nearly vertical nature of the magnetic field in auroral regions, Lorentz coupling involves a direct transfer of energy to the neutrals in a horizontal way [e.g., *Knudsen*, 1969; *Chimonas*, 1969]. Obviously, Lorentz force in equatorial regions is vertical due to the eastward electric field and the magnetic field is almost horizontal. An additional consideration is the strength of the magnetic field in auroral and equatorial regions. The magnetic field strength in auroral regions is approximately double that in the equatorial region and given that the current density magnitude in EEJ is about 1/3 that of the auroral electrojet (AEJ) during geomagnetic storms [*Akasofu et al.*, 1965; *Knudsen*, 1969], the resulting force ($\mathbf{J} \times \mathbf{B}$) in EEJ is smaller than that in auroral region by a factor of 1/5 [*Knudsen*, 1969; *Yizengaw et al.*, 2018]. Thus, the orientation of the Lorentz force, integrated current density in EEJ and AEJ and magnetic field strength influences the resultant energy transfered from ions to neutrals; and hence distinguishes the characteristics of the launched AGWs in auroral and equatorial regions. Therefore, even during geomagnetic storms, the Lorentz coupling involving EEJ changes is less effective in launching AGWs resulting into TIDs in equatorial regions compared to auroral regions [*Chimonas*, 1969]. There are other processes such as Joule heating and particle precipitation that are more effective in high latitudes compared to equatorial latitudes during geomagnetic storms [*Hocke and Schlegel*, 1996; *Hajkowicz and Hunsucker*, 1987]. While the $\Delta$TEC magnitudes associated with equatorward and poleward TIDs (where both exist) may be comparable in the shown examples, it doesn't directly mean that their amplitudes at the source origin are indeed similar. For-example, this study has shown that AGWs which give rise to poleward TIDs statistically propagate up to $10-30^{\circ}$ from the geomagnetic equator, while equatorward TIDs are detected even crossing the equator [e.g., *Balthazor and Moffett*, 1997; *Bruinsma and Forbes*, 2009]. During their propagation, equatorward AGWs/TIDs experience energy dissipation as they travel away from the source origin. The study by *Pradipta et al.* [2016] has reported results of high resul-



This article is protected by copyright. All rights reserved.

Author Manuscript

tant amplitudes of LS TIDs near the geomagnetic equator due to the interference of TIDs originating from the auroral regions during the geomagnetic storm of 26 September 2011. In future, it will be interesting to statistically establish and compare the range of amplitudes for AGWs/TIDs originating in equatorial and auroral regions during geomagnetic storms based on observational data.

## 4 Conclusions

In this study, we have established that poleward TIDs during geomagnetic storms over the African and American sectors occur mainly during local daytime. Over the African sector, the poleward TIDs during the main phase were mostly large scale with cases of periods greater or equal to 1 hour and velocity values of 300-550 m/s accounting for about 64% of the events. During the recovery phase of the storms, the observed poleward TIDs were dominated by the medium scale category (63%) with periods of less than an hour. For the American sector, poleward TIDs also occur predominantly during local daytime, although there are some cases observed during nighttime hours. Interestingly, most of the poleward TIDs over the American sector occurred during the storm main phase as opposed to the African sector that had a significant number of poleward TIDs during the recovery phase. Overall, electrodynamics related to enhanced eastward electric field and hence increased vertical $\mathbf{E} \times \mathbf{B}$ drift plays a crucial role in launching atmospheric gravity waves in equatorial latitudes which are a likely source of the reported poleward TIDs. This investigation found that there are more poleward TIDs over the African sector than the American sector during disturbed conditions. The reasons for this difference are not established in this paper and will be a future investigation. It is found that poleward TIDs over both African and American sectors are largely confined within $10-30^{\circ}$ of the geomagnetic equator.

**Acknowledgments**

EEJ data is available at http://magnetometers.bc.edu/index.php/downloads. AMBER is operated by The Aerospace Corporation and Boston College with funding from NSF and AFOSR. LISN is a project led by the University of Texas at Dallas in collaboration with the Geophysical Institute of Peru and other institutions that provide information for the benefit of the scientific community. Their data are available from http://lisn.igp.gob.pe website. The Dst and Kp indices data were accessed from the World Data Centre, Ky-



This article is protected by copyright. All rights reserved.

Author Manuscript

oto, Japan http://wdc.kugi.kyoto-u.ac.jp. This work is based on the research supported in part by the National Research Foundation of South Africa (Grant Numbers 112090 and 129285) and opinions, findings and conclusions or recommendations expressed in this paper are of the author(s), and the NRF accepts no liability whatsoever in this regard. Contributions of MBM were supported by the US National Science Foundation (AGS 1848724). EY's work has been partially supported by AFOSR (FA9550-20-1-0119) and NSF (AGS-1848730) and NSF AGS145136 grants.

## References

Akasofu, S.-I, S. Chapman, and C. -I Meng (1965), The polar electrojet, *J. Atmos. Terr. Phys.*, *27*(11-12), 1275–1300.

Anderson, D., A. Anghel, K. Yumoto, M. Ishitsuka, and E. Kudeki (2002), Estimating daytime vertical E×B drift velocities in the equatorial F-region using ground-based magnetometer observations, *Geophys. Res. Lett*, *29*(12), 1596, doi:10.1029/2001GL014562.

Anderson, D., A. Anghel, J. Chau, and O. Veliz (2004), Daytime vertical E× B drift velocities inferred from ground-based magnetometer observations at low latitudes, *Space Weather*, *2*(S11001), doi:10.1029/2004SW000095.

Balthazor, R. L., and R. J. Moffett (1997), A study of atmospheric gravity waves and traveling ionospheric disturbances at equatorial latitudes, *Ann. Geophys.*, *15*, 1048–1056.

Bruinsma, S. L., and J. M. Forbes (2009), Properties of traveling atmospheric disturbances (TADs) inferred from CHAMP accelerometer observations, *Adv. Space Res.*, *43*, 369–376.

Borries, C., N. Jakowski and V. Wilken (2009), Storm induced large scale TIDs observed in GPS derived TEC, *Ann. Geophys.*, *27*, 1605–1612.

Chimonas, G. (1969), The Upper Atmosphere in Motion: The Equatorial Electrojet as a source of long period traveling ionospheric disturbances, *Geophysical Monograph Series*, *18*, 698–706.

Ding, F., W. Wan, B. Ning, B. Zhao, Q. Lin, Y. Wang, L. Hu, R. Zhang, and B. Xiong (2013), Observations of poleward-propagating large-scale traveling ionospheric disturbances in Southern China, *Ann. Geophys.*, (31), 377–385.



This article is protected by copyright. All rights reserved.

Author Manuscript

Fejer, B. G., and L. Scherliess (1995), Time dependent response of equatorial ionospheric electric field to magnetospheric disturbances, *Geophys. Res. Lett.*, *22*(7), 851–854.

Habarulema, J. B., Z. T. Katamzi, E. Yizengaw, Y. Yamazaki and G. Seemala (2016), Simultaneous storm time equatorward and poleward large-scale TIDs on a global scale, *Geophys. Res. Lett.*, (43), 6678–6686.

Habarulema, J. B., Z. T. Katamzi, and E. Yizengaw (2015), First observations of poleward large-scale traveling ionospheric disturbances over the African sector during geomagnetic storm conditions, *J. Geophys. Res. Space Phys.*, (120), 6914–6929.

Habarulema, J. B., E. Yizengaw, Z. T. Katamzi-Joseph, M. B. Moldwin, and S. Buchert (2018), Storm time global observations of large-scale TIDs from ground-based and in situ satellite measurements, *J. Geophys. Res. Space Phys.*, (123), 711–724, https://doi.org/10.1002/2017JA024510.

Hajkowicz, L. A., and R. D. Hunsucker (1987), A simultaneous observation of large-scale periodic TIDs in both hemispheres following an onset of auroral disturbances, *Planet Space Science*, *35*(6), 785–791.

Hocke, K., and K. Schlegel (1996), A review of atmospheric gravity waves and traveling ionospheric disturbances, *Ann. Geophysicae*, *14*, 917–940.

Huang, C. M., A. D. Richmond, and M. -Q. Chen (2005), Theoretical effects of geomagnetic activity on low-latitude electric fields, *J. Geophys. Res.*, *110*, A05312, doi:10.1029/2004JA010994.

Hunsucker (1982), Atmospheric Gravity Waves Generated in the High-Latitude Ionosphere: A Review, *Reviews of Geophysics and Space Physics*, *20* (2), 293–315.

Jonah, O. F., A. Coster, L. G. S. Zhang, P. J. Erickson, E. R. de Paula and E. A. Kherani (2018), TID Observations and source analysis during the 2017 memorial day weekend geomagnetic storm over North America, *J. Geophys. Res. Space Physics*, *123*, 8749–8765, https://doi.org/10.1029/2018JA025367.

Katamzi, Z. T., and J. B. Habarulema (2014), Traveling ionospheric disturbances observed at South African midlatitudes during the 2931 October 2003 geomagnetically disturbed period, *Adv. Space Res.*, *53*, 48–62.

Kersley, L., and J. A. Hughes (1989), On the distinction between large scale and medium-scale atmospheric gravity waves, *Ann. Geophys.*, *7*, 459–462.



This article is protected by copyright. All rights reserved.

Author Manuscript

Kikuchi, T., H. Lühr, K. Schlegel, H. Tachihara, M. Shinohara and T. -I. Kitamura (2000), Penetration of auroral electric fields to the equator during a substorm, *J. Geophys. Res.*, *105*(A10), 23251–23261.

Knudsen, W. C (1969), Neutral Atmosphere Wave Generation by the Equatorial Electrojet, *J. Geophys. Res.*, *74*(16), 4191–4192.

Liu, J., D. -H. Zhang, A. J.Coster, S. -R. Zhang, G. -Y. Ma, Y. -Q. Hao and Z. Xiao (2019), A case study of the large-scale traveling ionospheric disturbances in the eastern Asian sector during the 2015 St. Patrick's Day geomagnetic storm, *Ann. Geophys.*, *37* (4), 673–687.

Ngwira, C. M., J. B. Habarulema, E. Astafyevar, E. Yizengaw, O. F. Jonah, G. Crowley, A. Gisler and V. Coffey (2019), Dynamic response of ionospheric plasma density to the geomagnetic storm of 22-23 June 2015, *J. Geophys. Res. Space Physics*, *124*, https://doi.org/10.1029/2018JA026172.

Nicolls, M. J., M. C. Kelley, A. J. Coster, S. A González and J. Makela (2004), Imaging the structure of a large-scale TID using ISR and TEC data, *Geophys. Res. Lett.*, *31*(L09812), doi:10.1029/2004GL019797.

Pradipta, R., C. E. Valladares, B. A. Carter, and P. H. Doherty (2016), Inter-hemispheric propagation and interactions of auroral traveling ionospheric disturbances near the equator, *J. Geophys. Res. Space Physics*, *121*, 2462–2474, doi:10.1002/2015JA022043.

Rastogi, R. G., and J. A. Klobuchar (1990), Ionospheric electron content within the equatorial F2 layer anomaly belt, *J. Geophys. Res.*, *95* (A11), 19045–19052.

Shiokawa, K., Y. Otsuka, T. Ogawa, N. Balan, K. Igarashi, J. Ridley, J. Knipp, A. Saito and K. Yumoto (2002), A large-scale traveling ionospheric disturbance during the magnetic storm of 15 September 1999, *J. Geophys. Res.*, *107*(A6), 10.1029/2001JA000245.

Thaganyana, G. P., J. B. Habarulema, C. Ngwira and I. Azeem (2021), Equatorward large-scale travelling ionospheric disturbances of high latitude origin during quiet conditions, *J. Geophys. Res. Space Physics*, Under Review.

Tsugawa, T., A. Saito, Y. Otsuka and M. Yamamoto (2003), Damping of large-scale traveling ionospheric disturbances detected with GPS networks during the geomagnetic storm, *J. Geophys. Res.*, *108*(A3),1127, doi:10.1029/2002JA009433.



This article is protected by copyright. All rights reserved.

Author Manuscript

Tsugawa, T., A. Saito, and Y. Otsuka (2004), A statistical study of large scale traveling ionospheric disturbances using the GPS network in Japan, *J. Geophys. Res.*, *109*(9), doi:10.1029/2003JA010302.

Valladares, C. E., J. Villalobos, M. A. Hei, R. Sheehan, S. Basu, E. MacKenzie, P. H. Doherty, and V. H. Rios (2009), Simultaneous observation of traveling ionospheric disturbances in the Northern and Southern Hemispheres, *Ann. Geophys.*, *27*, 1501–1508.

Valladares, C. E., and J. L. Chau (2012), The Low-Latitude Ionosphere Sensor Network: Initial results, *Radio Sci.*, *47*(RS0L17), doi:10.1029/2011RS004978.

Valladares, C. E., and M. A. Hei (2012), Measurement of the characteristics of TIDs using small and regional networks of GPS receivers during the campaign of 17-30 July of 2008, *Int. J. Geophys.*, *548784*(2012), doi:10.1155/2012/548784.

Yizengaw, E., and M. B. Moldwin (2009), African Meridian B-field Education and Research (AMBER) Array, *Earth, Moon, and Planets*, doi:10.1007/s11038-008-9287-2.

Yizengaw, E., E. Zesta, M. B. Moldwin, M. Magoun, N. K. Tripathi, C. Surussavadee, and Z. Bamba (2018), ULF wave-associated density irregularities and scintillation at the equator, *Geophys. Res. Lett.*, *45*, 5290–5298, https://doi.org/10.1029/2018GL078163.

Yizengaw, E., M. B. Moldwin, A. Mebrahtu, B. Damtie, E. Zesta, C. E.Valladares, and P. H. Doherty (2011), Comparison of storm time equatorial ionospheric electrodynamics in the African and American sectors, *J. Atmos. Solar-Terr. Phys.*, *73*(1), 156–163.

Yizengaw, E., E. Zesta, M. B. Moldwin, B. Damtie, A. Mebrahtu, C. E. Valladares, and R. F. Pfaff (2012), Longitudinal differences of ionospheric vertical density distribution and equatorial electrodynamics , *J. Geophys. Res. Space Phys.*, *A07312*, doi:10.1029/2011JA017454.

## Figure captions

Figure 1: Distribution of GNSS receivers used in the study (a) and examples of poleward TIDs occurrence over the African sector on (b) 16 July 2012, (b) 14 April 2014 and (d) 16 November 2014.



This article is protected by copyright. All rights reserved.

Author Manuscript

Figure 2: Similar to Figure 1; for the American sector on (b) 02 October 2013, (c) 15 July 2013, and (d) 02 March 2017.

Figure 3: Statistical results of poleward TIDs during main and recovery phases for geomagnetic storms which occurred from 2010-2018 over the African sector.

Figure 4: Similar to Figure 3 but for the American sector.

Figure 5: An example showing the procedure followed to establish the correlation between occurrence of poleward TIDs and changes in EEJ variability as (a) $\Delta$TEC (TECU) over the African sector on 11 March 2012, (b) $\Delta$H (nT) for 11 March 2012 and corresponding monthly median $\Delta$H (nT) for March 2012. In (c), a scatter plot of estimated start time of poleward TIDs and time of maximum $\Delta$H during the period when poleward TIDs existed is shown.

Figure 6: $\Delta$TEC and $\Delta$H variability on 16 July 2012 over the African sector showing poleward TIDs at 0700 UT when $\Delta$H values were largely negative.

Figure 7: Similar to Figure 5 over the American sector. The example showing the occurrence of poleward TIDs and increase in EEJ over monthly median values is shown for 02 March 2017. In panel (c), a scatter plot of estimated start time of poleward TIDs and time of maximum $\Delta$H during the period when poleward TIDs existed is shown using derived EEJ with two pairs of magnetometers ALTA-CUIB (black dots) and JICA-PIUR (red crosses).



This article is protected by copyright. All rights reserved.

Author Manuscript

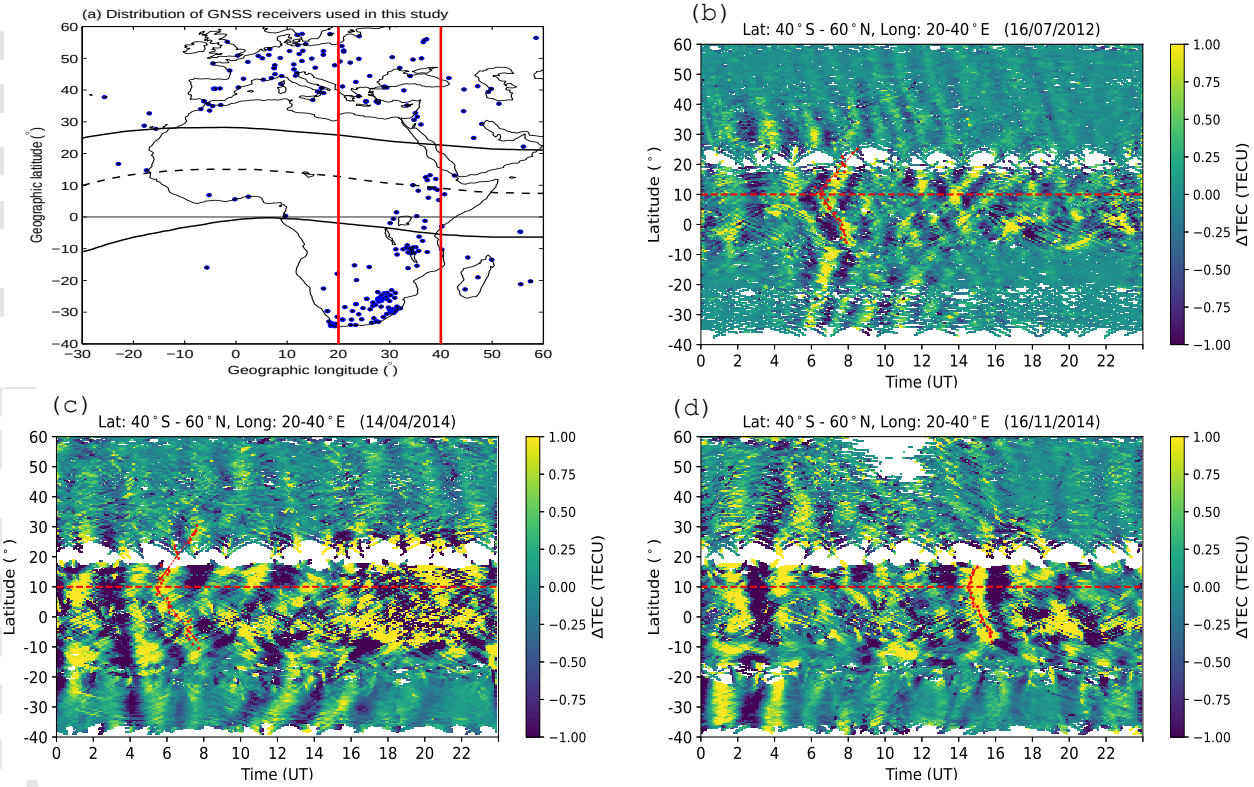


This article is protected by copyright. All rights reserved.

Author Manuscript

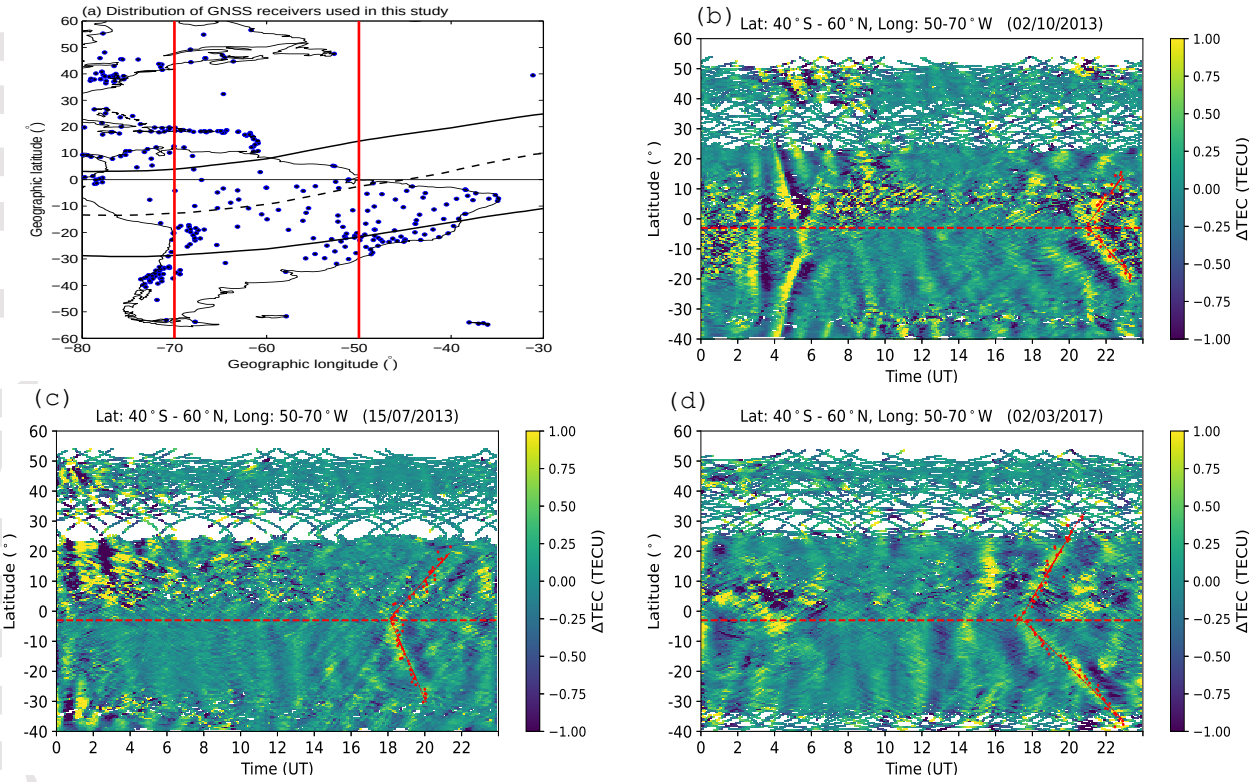


This article is protected by copyright. All rights reserved.

Author Manuscript

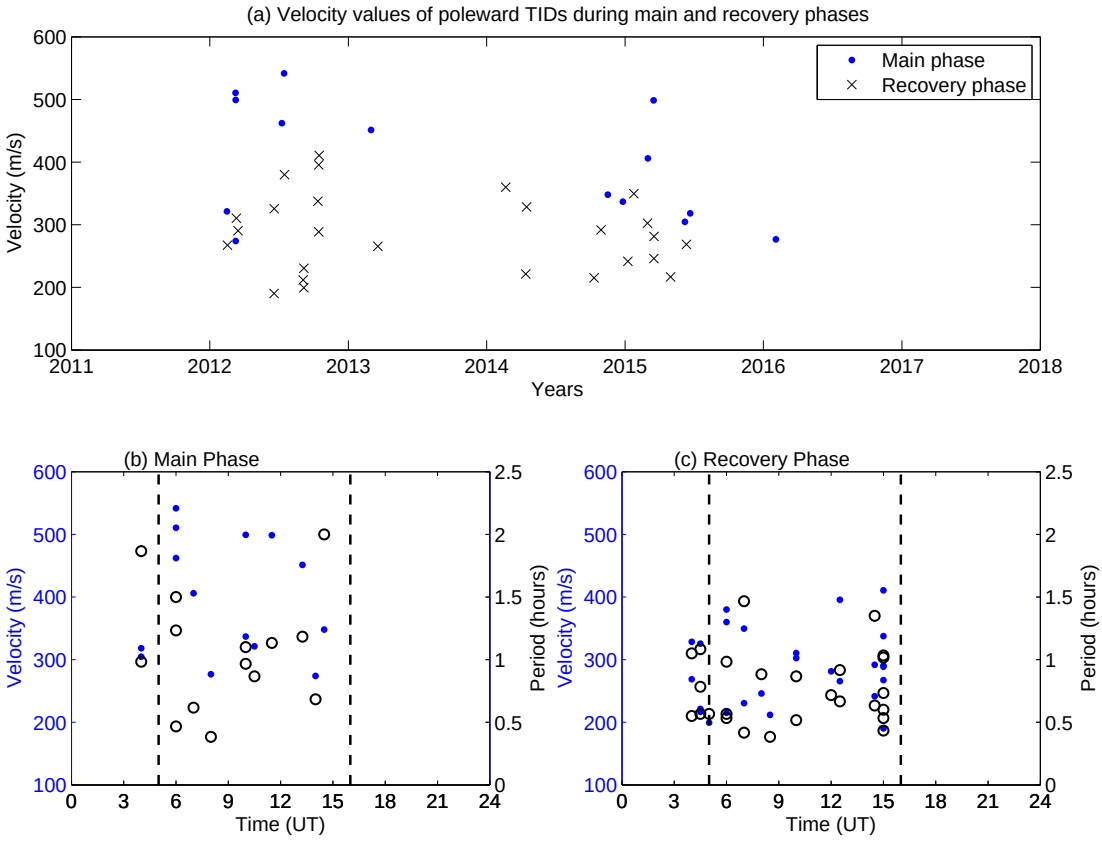


This article is protected by copyright. All rights reserved.

Author Manuscript

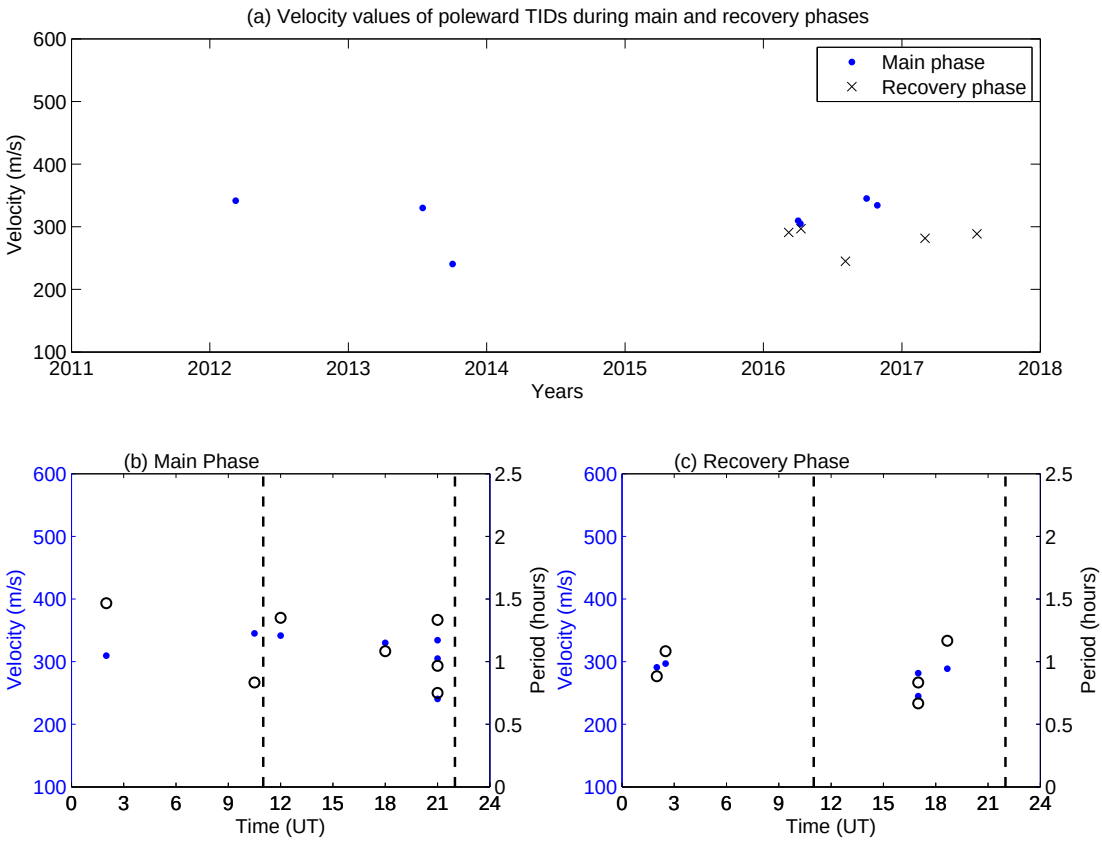


This article is protected by copyright. All rights reserved.

Author Manuscript

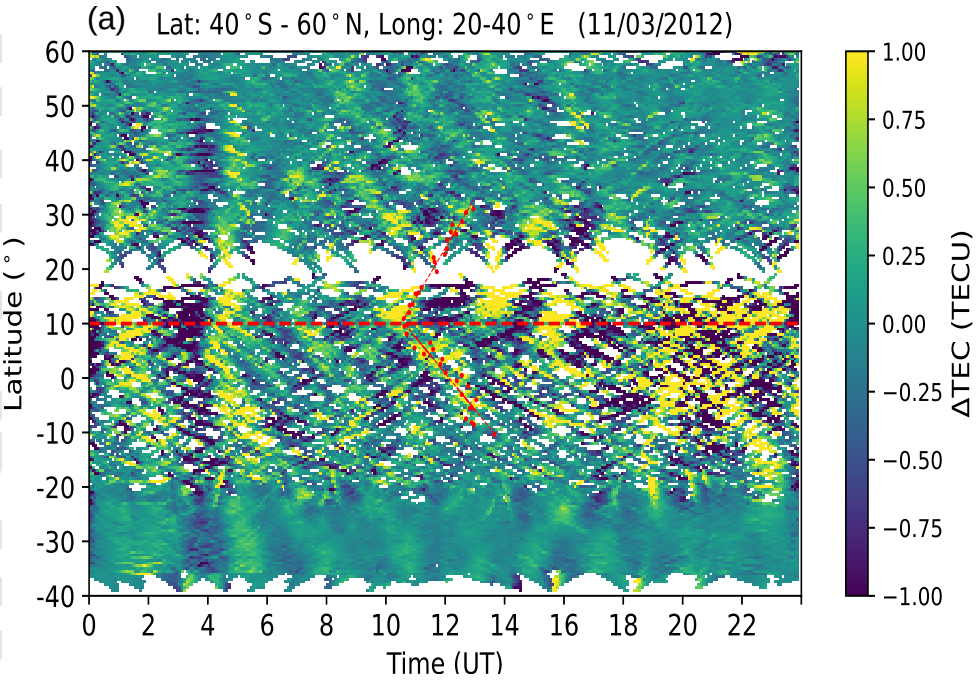


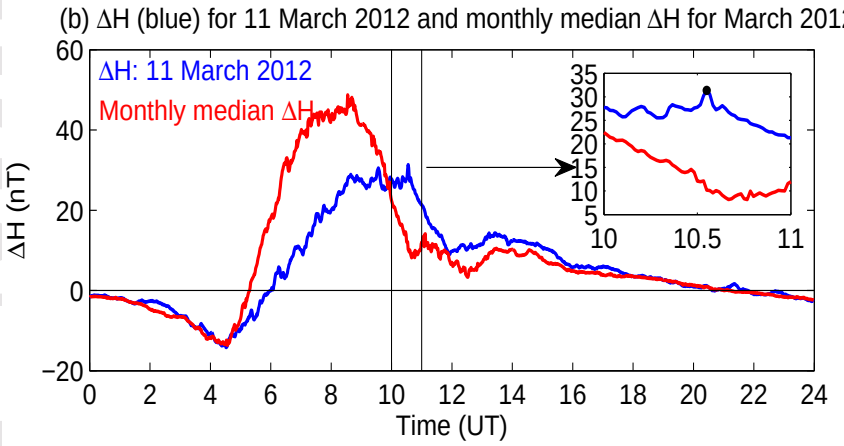


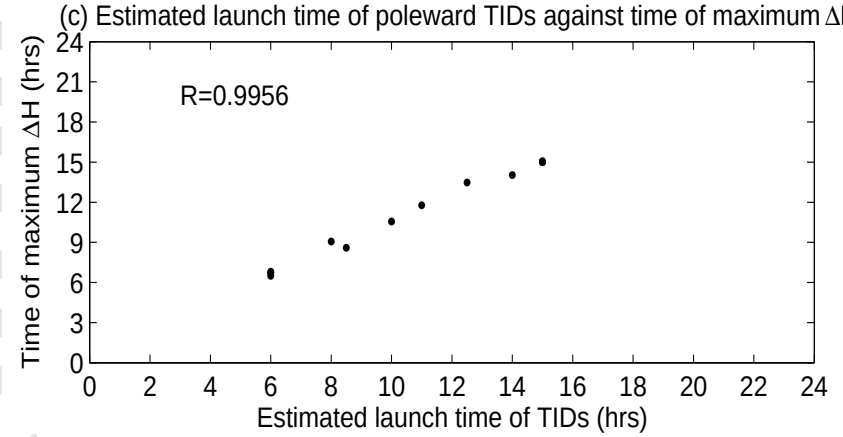


This article is protected by copyright. All rights reserved.

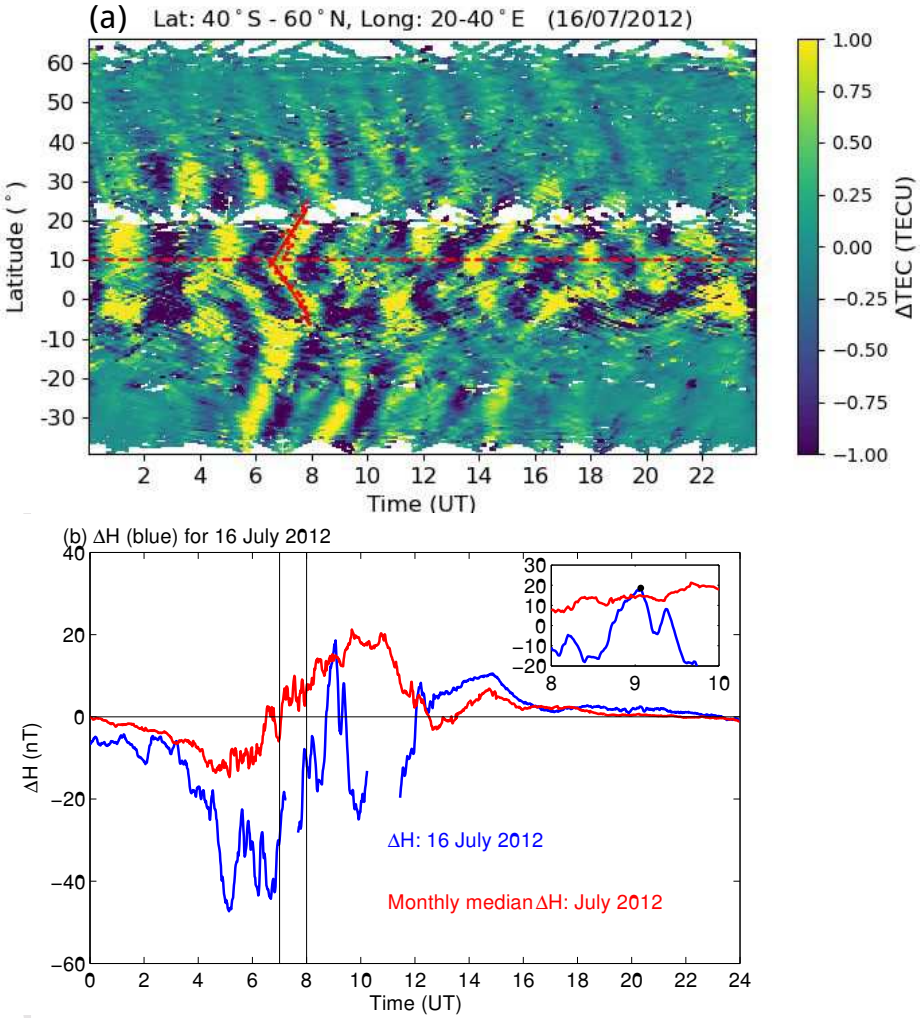


Author Manuscript

This article is protected by copyright. All rights reserved.

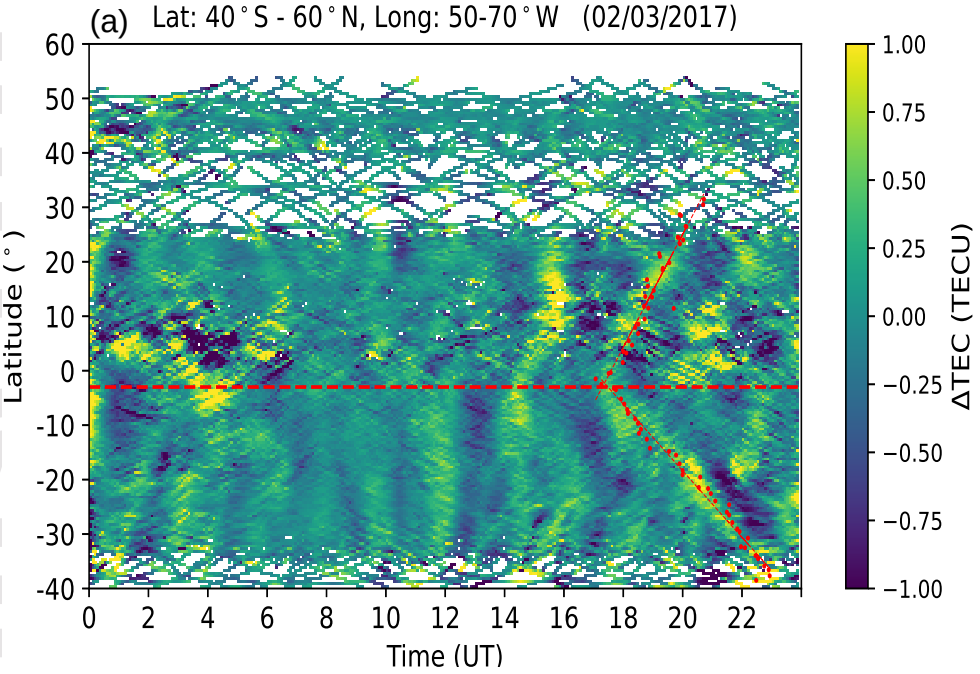


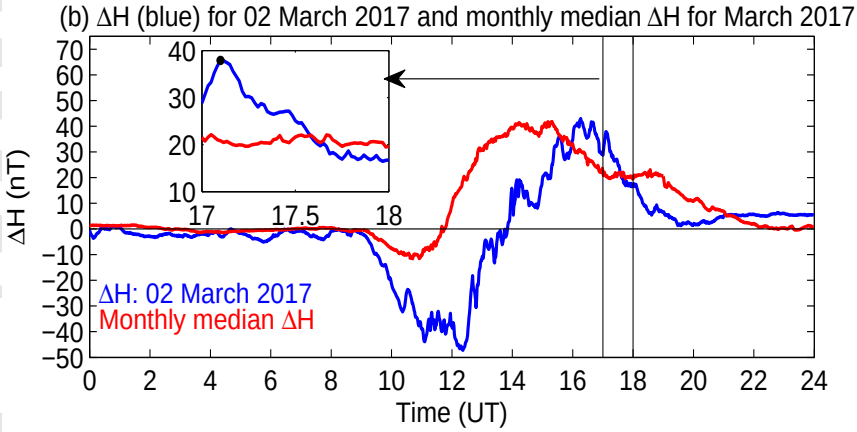


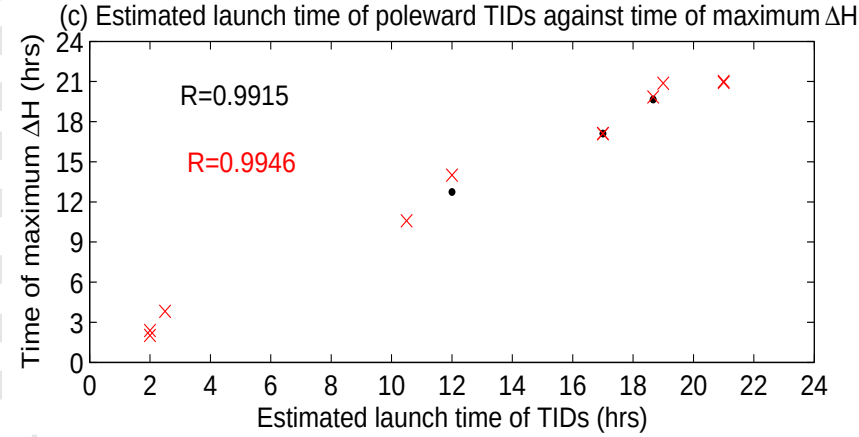


This article is protected by copyright. All rights reserved.